

# Phase behaviour of poly( $\epsilon$ -caprolactone)/poly(styrene-*ran*-acrylonitrile) blends exhibiting both liquid-liquid unmixing and crystallization

K. Schulze, J. Kressler\* and H. W. Kammer†

Dresden University of Technology, Department of Macromolecular Chemistry and Textile Chemistry, Mommsenstrasse 13, D-8027 Dresden, Germany

(Received 8 June 1992; revised 18 December 1992)

Miscibility and morphology in blends of poly( $\epsilon$ -caprolactone) (PCL) and poly(styrene-*ran*-acrylonitrile) (SAN) were examined by light scattering and optical microscopy. The blends display miscibility in the amorphous state in a limited range of copolymer composition. Morphologies, formed as a combined effect of liquid-liquid phase separation and crystallization of PCL, are discussed. Crystallization leads to spherulite structure in the blends. Upon crystallization, PCL segregates from the amorphous state resulting in the observation of ring patterns in miscible blends. Its periodicity decreases with increasing fraction of SAN in the blend. Ring-banded spherulites have not been observed in neat PCL or in immiscible blends. These effects are discussed in terms of twisted crystallization.

(Keywords: blends; poly( $\epsilon$ -caprolactone); phase behaviour; spherulites; phase separation)

## INTRODUCTION

Phase separation phenomena present the possibility of morphology control in polymer blends. It is especially interesting to study the combined effect of liquid-liquid phase separation and crystallization. Morphology control by these two phase transitions was also performed in forced mixtures of isotactic polypropylene and ethylene-propylene random copolymers<sup>1,2</sup>. Another example of the competition of different phase transitions is the interplay of liquid-liquid, liquid-solid phase transition and the formation of an anisotropic phase in blends of poly(ethylene terephthalate) and a liquid crystalline copolyester<sup>3-5</sup>. Different kinds of phase transitions may increase the complexity of the morphology of these polymer blends.

In the present study, the phase behaviour and resulting morphologies in blends of poly( $\epsilon$ -caprolactone) (PCL) and random copolymers of styrene and acrylonitrile (code: SAN-*x*, *x*=wt% of AN) are investigated. It is well known that PCL and SAN are miscible only in a limited range of copolymer composition<sup>6</sup>, i.e. the blends display a window of miscibility in the temperature-copolymer composition plane. Near the borderline of miscibility/immiscibility, phase separation at elevated temperatures (lower critical solution temperature, *LCST*, behaviour) can be observed. Moreover, PCL is a semicrystalline polymer, therefore a maximum of melting point

depression inside the window of miscibility at about 19 wt% AN was found<sup>7</sup>.

Liquid-liquid phase separation above *LCST* results in regular phase patterns. Subsequent crystallization transfers the PCL-rich domains into 'spherulitic' domains. Thus, the superposition of spinodal decomposition and crystallization can be studied.

In blends involving a crystallizable and an amorphous component one has to recognize that the morphology may be influenced by the thermal history of the system. The crystallization of PCL in the blend is accompanied by phase separation for blends inside the window of miscibility. Consequently, a complicated morphology arises which depends strongly on the PCL content.

In the following, the phase behaviour and morphological features in blends of the title polymers will be discussed.

## EXPERIMENTAL

### Materials

The PCL used in this study was supplied by Union Carbide Corp. (PCL-700). The copolymerization of SAN was carried out at 60°C in ethylbenzene with an AIBN concentration of 0.02 mol l<sup>-1</sup>. The maximum degree of conversion<sup>8</sup> amounted to about 6%. Molecular characteristics of the polymers are listed in Table 1.

### Blend preparation

Both polymers were dissolved in 1,2-dichloroethane (5 wt% of total polymer). For microscopy and light scattering the samples were cast onto a cover glass. All samples were subsequently dried for 2 days at 60°C in a vacuum oven.

\* Present address: Department of Organic and Polymeric Materials, Tokyo Institute of Technology, Ookayama, Meguro-ku, Tokyo 152, Japan

† To whom correspondence should be addressed

### Equipment

For cloud point measurements the samples were heated in a hot-stage (Linkam 600) and the scattering intensity of laser light (647 nm) was measured under an angle of 20° by a photo cell. Light microscopy was carried out with a Jenapol microscope (Carl-Zeiss-Jena).

## RESULTS AND DISCUSSION

### Phase behaviour

As reported previously<sup>6</sup> the miscibility window of SAN/PCL blends ranges from 8 to 28 wt% AN in SAN. Furthermore, PCL crystallizes below about 60°C. The results depicted in Figure 1 for SAN/PCL 70/30 blends agree well with those of ref. 6. It can be seen that near the edges of the miscibility window, LCST-type coexistence curves are detected. The miscibility window is designed from cloud points (solid circles) and by optical inspection of solution-cast films at room temperature which remained opaque and transparent, respectively, upon heating. In the heterogeneous region and at the edges of the miscibility window the SAN/PCL 70/30 blends are able to crystallize in a reasonable time scale (open circles represent the melting points) whereas in the centre of the miscibility window the crystallization is extremely retarded.

In the centre of the miscibility region the phase

**Table 1** Values of molecular weights  $M_w$ , polydispersity  $M_w/M_n$  and number of segments  $r$  of SAN copolymers

Copolymer composition		$M_w$ (g mol <sup>-1</sup> )	$M_w/M_n$	$r$
wt% AN	mol% AN			
PCL	—	40 400	2.61	354
9.4	16.9	128 000	1.97	1290
9.8	17.6	135 000	2.18	1360
12.9	22.5	154 000	2.08	1580
19.2	31.8	166 000	2.21	1760
27.0	42.1	167 000	2.04	1850
28.2	43.5	178 000	2.14	1990
30.5	46.3	186 000	2.02	2100
34.4	50.7	179 000	1.97	2070

separation temperature exceeds the temperature of thermal decomposition and is not accessible experimentally. This effect has often been observed in copolymer containing blends and is sometimes called the 'miscibility chimney'<sup>9</sup>. The phase behaviour of the blends is listed in Table 2 in dependence on the copolymer composition.

Liquid-liquid phase separation presented in Figure 1 and Table 2 can be rationalized in the context of an equation-of-state theory<sup>10,11</sup>. According to that theory the spinodal is given by:

$$\frac{1}{r_A \phi_A} + \frac{1}{r_B \phi_B} - 2X = 0 \quad (1)$$

where  $r_i$  and  $\phi_i$  denote the degree of polymerization and the volume fraction of component  $i$ , respectively. The free energy parameter  $X$  reads<sup>11</sup>:

$$X = 2 \frac{\tilde{V}_A^{1/3}}{\tilde{V}_A^{1/3} - 1} X_{AB} + \frac{\tilde{V}_A^{1/3}}{\frac{4}{3} - \tilde{V}_A^{1/3}} \frac{7}{8} \Gamma^2 \quad (2)$$

where  $\tilde{V}_A$  is the reduced volume of component A taken to be the reference substance. The overall interaction parameter  $X_{AB}$  and the free volume parameter  $\Gamma$  can be expressed by individual segmental-based quantities for a blend comprising a random copolymer. It follows, when A = PCL and B = SAN:

$$X_{AB} = \beta \chi_{CL/S} + (1 - \beta) \chi_{CL/AN} - \beta(1 - \beta) \chi_{S/AN}$$

$$\Gamma = \beta \delta_S + (1 - \beta) \delta_{AN} - 2\beta(1 - \beta) \chi_{S/AN} \quad (3)$$

**Table 2** Phase separation temperature in dependence on the copolymer composition for SAN/PCL 70/30 blends

wt% AN in SAN	Phase separation temperature (°C)
9.4	Immiscible
9.8	128
12.9	Miscible up to thermal decomposition
26.5	Miscible up to thermal decomposition
27.0	227
27.5	228
28.2	223
30.5	139
34.4	Immiscible

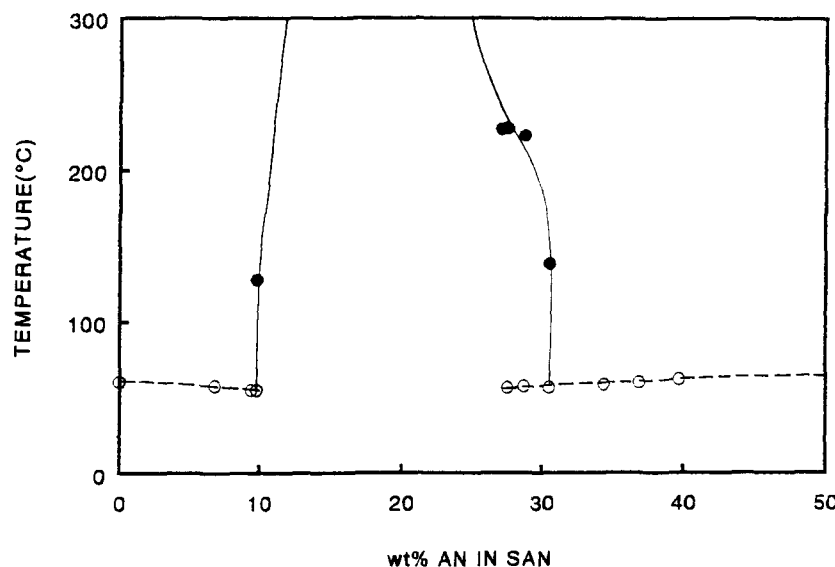


**Figure 1** Window of miscibility of SAN/PCL 70/30 (wt%) blends. Miscibility occurs only in the region inside the solid curves above the melting points: ●, cloud points; ○, melting points

where  $\beta$  is the mole fraction of styrene in SAN;  $\chi_{ij}$  represents the interaction parameter between segments of type  $i$  and  $j$  and  $\delta_i$  stands for:

$$\delta_i \equiv \frac{T_i^*}{T_A^*} - 1 \quad (4)$$

where  $T^*$  is the respective reference temperature. It can be calculated by applying Flory's equation of state<sup>12</sup>:

$$\tilde{T} = \frac{\tilde{V}^{1/3} - 1}{\tilde{V}^{4/3}} \quad (5)$$

in combination with

$$\tilde{V}^{1/3} - 1 = \frac{\alpha T}{3(1 + \alpha T)} \quad (5')$$

$\alpha$  being the thermal expansion coefficient. As indicated above, the homopolymer PCL is chosen as reference substance A. The thermal expansion coefficient has been reported<sup>13</sup> to be  $\alpha = 7.2 \times 10^{-4} \text{ K}^{-1}$  in the range 80–130°C. Using this value, from equations (5) and (5') one obtains  $T_{\text{PCL}}^* = 7200 \text{ K}$  as a reasonable value. The reference temperatures  $T_{\text{PS}}^* = 8300 \text{ K}$  and  $T_{\text{PAN}}^* = 9150 \text{ K}$  and the interaction parameter  $\chi_{\text{S/AN}} = 0.12$  have been reported elsewhere<sup>14</sup>. Hence, all quantities occurring in equations (1)–(3) are known except  $\chi_{\text{CL/S}}$  and  $\chi_{\text{CL/AN}}$ . Using the respective temperatures of phase decomposition at the borderlines of the miscibility window at 9.8 ( $\beta = 0.824$ ) and 30.5 ( $\beta = 0.537$ ) wt% AN, respectively, one arrives at

$$\chi_{\text{CL/S}} = 7.7 \times 10^{-3} \text{ and } \chi_{\text{CL/AN}} = 0.049 \quad (6)$$

The parameters involved in equation (3) are summarized in Table 3.

### Morphology formation

**Liquid–liquid phase separation.** Blends displaying both liquid–liquid phase separation and crystallization convey the possibility for superposition of these two phenomena which may result in interesting morphologies. Liquid–liquid (l–l) phase separation in the thermodynamically unstable region proceeds via spinodal decomposition which results in bicontinuous periodic two-phase morphologies having a characteristic spacing  $d$ . In the course of phase separation  $d$  increases. Subsequent quenching leads to spherulites of size  $D$ . When the l–l phase separation progresses only for a short time, the composition of both phases does not differ very much and crystallization of PCL is almost inhibited. With increasing period of l–l phase decomposition, however, PCL-rich and SAN-rich phases are formed. After quenching, many nuclei are formed in the PCL-rich regions which grow to spherulites. Hence, the PCL-rich regions are transferred to 'spherulitic' domains where  $D < d$ . The periodic phase decomposition structure resulting from spinodal decomposition then consists of

spherulitic and amorphous regular domains. These effects can be seen in Figure 2. When crystallization also progresses in the PCL-poor phase, the morphological features resulting from spinodal decomposition will be erased after a certain period of time. This is demonstrated in Figure 3. The process, of course, is promoted by the fact that the glass transition temperature ( $T_g$ ) of the blend is not far above room temperature.

**Ring-banded spherulites.** Figure 4 shows spherulites as they are formed in miscible and immiscible blends. In the immiscible system, SAN is segregated (small black spots in Figure 4b) while it is rejected into interlamellar regions in the miscible system. Ring-banded spherulites were not observed in neat PCL nor in immiscible blends comprising PCL. However, regular ring patterns can occur in miscible PCL-based blends that contain an amorphous component<sup>15–18</sup>. Morphological studies reveal that in these blends the amorphous mixture is included within the spherulites and confined to interlamellar regions. Lamellae are formed by PCL.

Distinct ring patterns in miscible blends can only be observed under certain crystallization conditions. Such morphologies are observed when (i) an amorphous component is present or (ii) there is a sufficiently high rate of crystallization compared to the mobility of the amorphous constituents. The second effect has been reported previously<sup>18</sup>. It is also seen in Figure 5. The periodicity of the rings varies with crystallization temperature. At high temperatures the structure of spherulites becomes disordered. As a result, the ring pattern is more irregular (Figure 5b). However, these fluctuations in periodicity are reduced when the SAN content increases. The periodic spacing seems to increase with increasing temperature<sup>15</sup>. Under constant crystallization conditions the spacing of the ring pattern also varies with blend composition. This is shown in Figure 6. The periodicity of the ring pattern decreases with decreasing PCL content. Similar results have been reported for blends of PCL with poly(vinyl chloride) and SAN (refs 16 and 17, respectively). The effect is more pronounced for blends comprising SAN with a composition near the edge of the miscibility area. Here, again the structure of the spherulites is disorganized with increasing SAN content, which ultimately results in no rings being observed.

The most comprehensive study on ring-banded spherulite structures in homopolymers such as polyethylene or polypropylene has been published by Keith and Padden<sup>19</sup>. The proposed basic mechanism leading to the ring pattern is axial twisting in lamellae under the influence of surface stresses, and cooperative arrangement of the twisted crystallites. The formation of ring-banded spherulites, displaying a high regularity, in miscible blends with PCL may be supported by an additional mechanism which becomes operative only in miscible blends.

When crystallization of PCL in the blend occurs, SAN with high  $T_g$  is rejected from the crystalline regions. In other words, the mobility of SAN molecules is low. This phenomenon may impose a transient non-uniform osmotic pressure on the growing crystallite which in turn results in a torque being imposed on it. Owing to the fact that periodicity in the ring pattern is the result of cooperative arrangements of twisted lamellae, a detailed theory of this mechanism is not straightforward.

Table 3 Reference temperatures and individual parameters for the system PCL/SAN

Polymer	$T^*$ (K)	$\chi_{\text{CL/S}}$	$\chi_{\text{CL/AN}}$	$\chi_{\text{S/AN}}$
PCL	7200	$7.7 \times 10^{-3}$	0.049	0.12
PS	8300		$\delta_{\text{S}} = 0.153$	
PAN	9150		$\delta_{\text{AN}} = 0.271$	

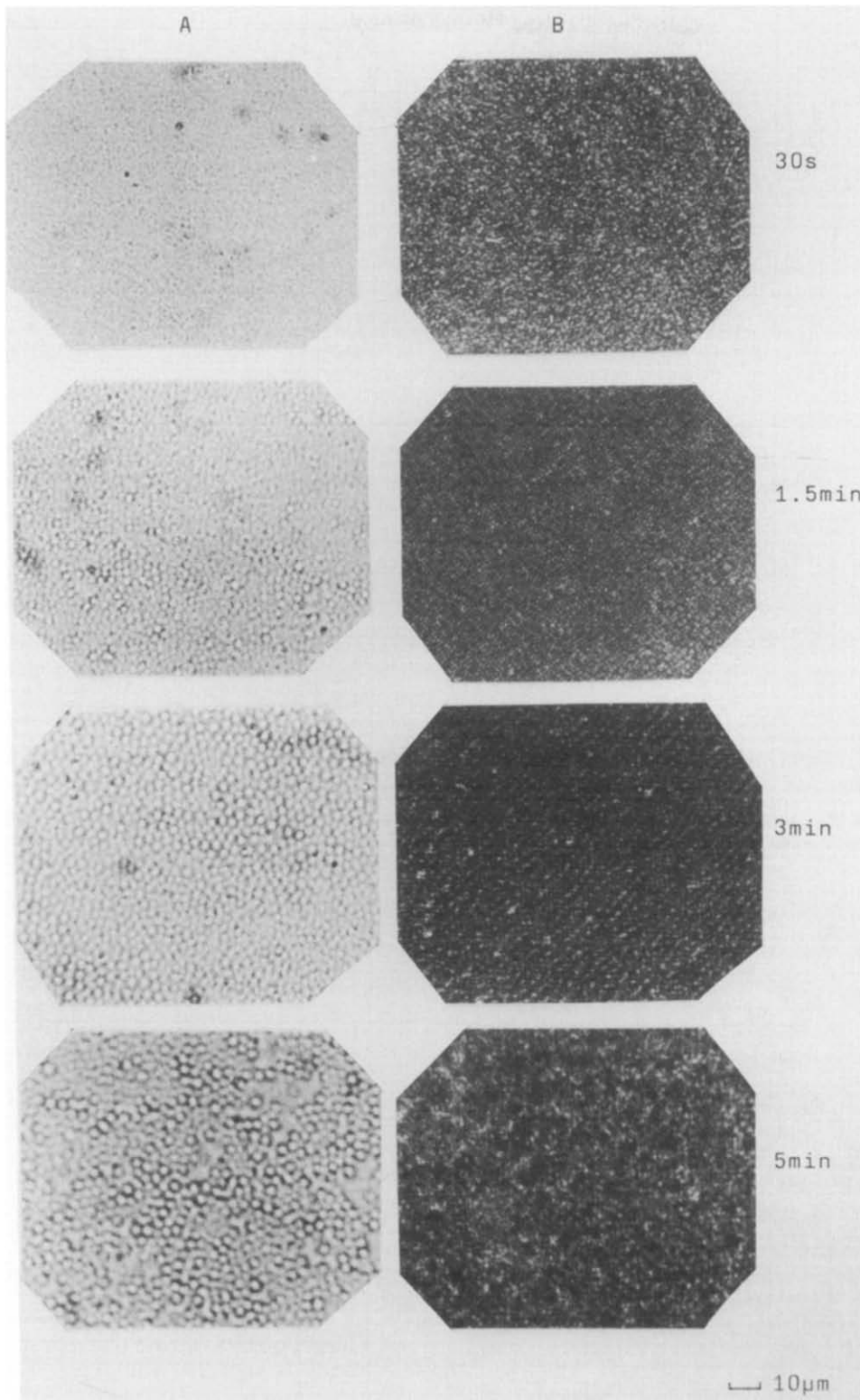


**Figure 2** Optical micrographs of SAN-26.5/PCL 40/60 blends. The samples were phase-separated at 260°C for the indicated periods of time, then rapidly quenched to room temperature and crystallized for 24 h. A, parallel polars; B, crossed polars

However, a simple scaling analysis can be helpful. Apart from all numerical factors, the periodic spacing  $L$  may scale as:

$$L \sim x^{m'} \quad (7)$$

with  $x \equiv p^*/p_{\text{osm}}$  and a scaling exponent  $m'$ ;  $p_{\text{osm}}$  and  $p^*$  are the osmotic pressure and some constant reference pressure, respectively. Using standard expressions for the

osmotic pressure, it follows that:

$$p_{\text{osm}} \sim -\frac{\ln(1-\phi)}{r} - X\phi^2 \approx -X\phi^2 \quad (8)$$

where  $X$  and  $\phi$  represent the free energy parameter of equation (2) and the volume fraction of SAN in the blend, respectively. The last expression of equation (8) results for a sufficiently high degree of polymerization,  $r$ .

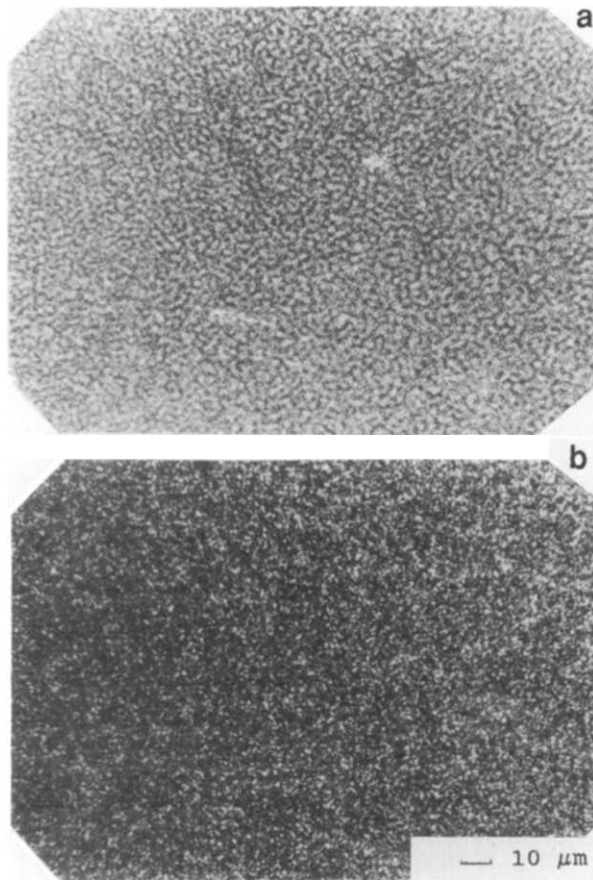


Figure 3 Same samples as in Figure 2, but phase-separated for 3 min, then crystallized for (a) 1 day and (b) 14 days

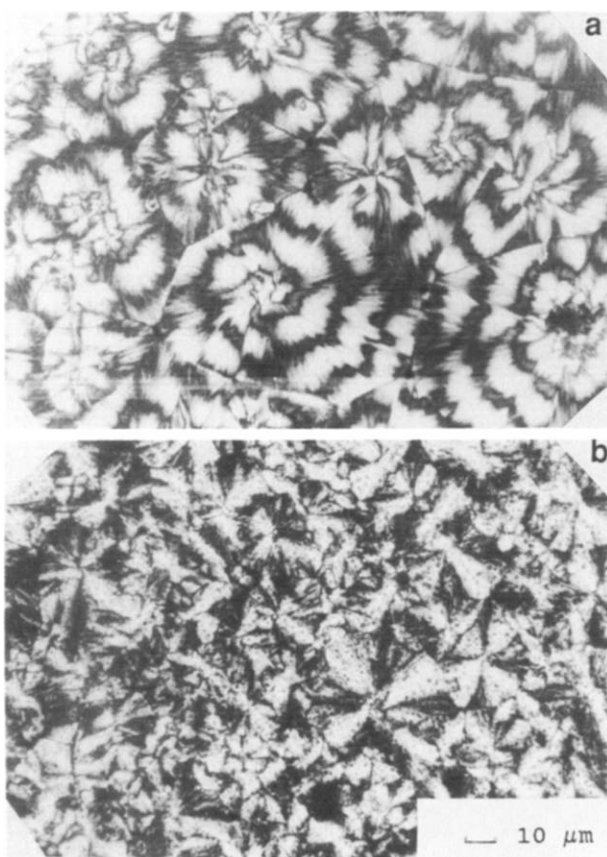


Figure 4 Optical micrographs of films of SAN/PCL 20/80 blends crystallized at 40°C: (a) miscible system with SAN-19.2; (b) immiscible system with SAN-9.4

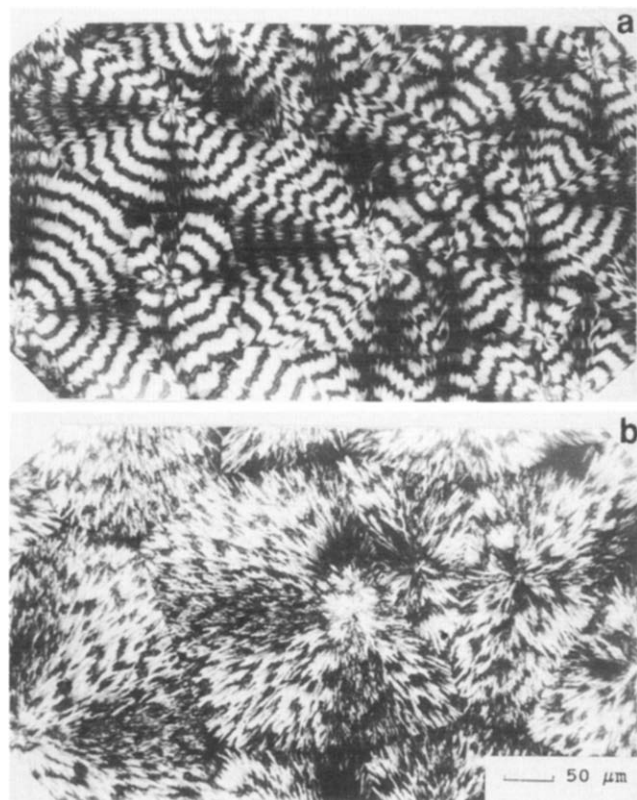


Figure 5 Optical micrographs of SAN-19.2/PCL 10/90 blends crystallized at (a) 45°C and (b) 50°C

Inserting equation (8) into relation (7), one arrives at:

$$L \sim \frac{1}{(\phi \sqrt{-X})^m} \quad (9)$$

Experimental results of Figure 6 and the scaling function (9) are compared in Figure 7. The interaction parameter  $-X$  was calculated according to equations (2) to (6). Values of 0.14 and 0.10 were obtained for PCL/SAN-19.2 and PCL/SAN-26.5, respectively. It is seen that the scaling function of equation (9) fits reasonably well with experimental data points. The scaling exponent itself turns out to be a function of the interaction parameter:

$$m \sim (-X)^{-1} \quad (10)$$

The following conclusions can be drawn from equations (9) and (10).

- (i) The periodicity of ring patterns in miscible polymer blends is reduced with increasing fraction of the non-crystalline component.
- (ii) The periodicity increases with increasing absolute value of the free energy parameter  $X$  since  $\frac{\partial L}{\partial (-X)} > 0$  after equations (9) and (10).

Both conclusions are in conformity with experimental results. Moreover, the formation of ring-banded spherulites in miscible blends is governed by a subtle balance of crystallization rate and diffusion rate which in turn influences the torque imposed on the growing crystallites. Hence, this phenomenon depends strongly on the difference of crystallization temperature and  $T_g$  of the amorphous constituents rejected from the crystalline

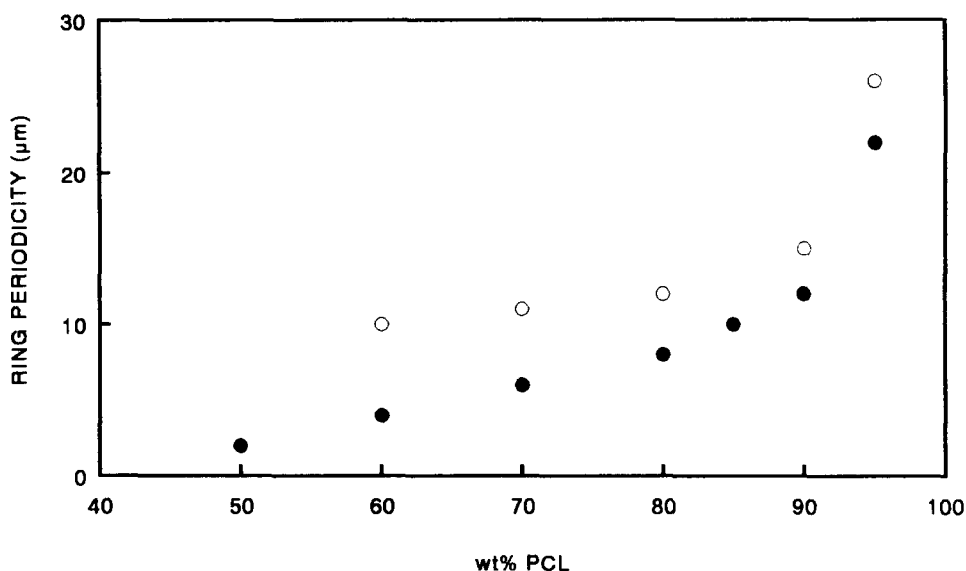


Figure 6 Variation of periodicity of the ring pattern with blend composition for two SAN/PCL blends crystallized at 40°C for 1 h: ○, 19.2 wt% AN in SAN; ●, 26.5 wt% AN in SAN

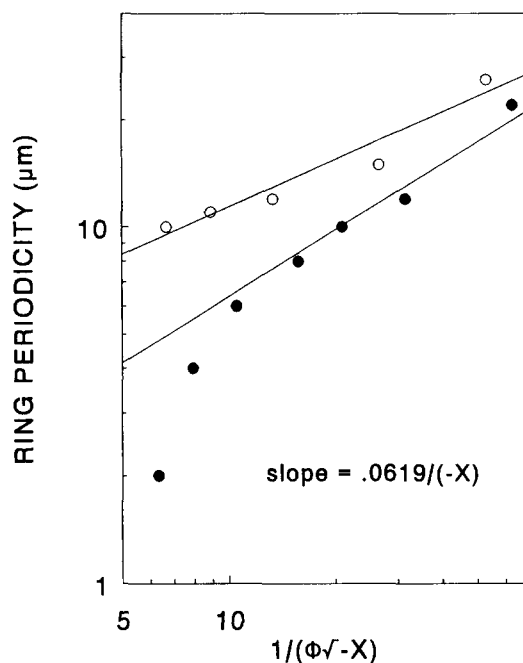


Figure 7 Scaled periodicity of ring pattern according to equation (9) (solid lines);  $\phi$  refers to the volume fraction of SAN in the blend. Experimental data points as in Figure 6

regions. When this difference is sufficiently small, the rate of crystallization slows down while the mobility of the amorphous component increases. As a result, the band

period increases and the ring patterns become more irregular.

## REFERENCES

- 1 Inaba, N., Sato, K., Suzuki, S. and Hashimoto, T. *Macromolecules* 1986, **19**, 1690
- 2 Inaba, N., Yamada, T., Suzuki, S. and Hashimoto, T. *Macromolecules* 1988, **21**, 407
- 3 Naleai, A., Shiwaku, T., Hasegawa, H. and Hashimoto, T. *Macromolecules* 1986, **19**, 3008
- 4 Nagaya, T., Orihara, H. and Ishibashi, Y. *J. Phys. Soc. Jpn* 1989, **58**, 3600
- 5 Kammer, H. W., Kressler, J., Kummerlöwe, C. and Morgenstern, B. *Polimery (Poland)* 1990, **35**, 199
- 6 Chiu, S. C. and Smith, T. G. *J. Appl. Polym. Sci.* 1984, **29**, 1797
- 7 Kressler, J. and Kammer, H. W. *Polym. Bull.* 1988, **19**, 283
- 8 Suess, M., Kressler, J. and Kammer, H. W. *Polymer* 1987, **28**, 957
- 9 Lath, D. and Cowie, J. M. G. *Makromol. Chem., Macromol. Symp.* 1988, **16**, 103
- 10 Kammer, H. W. *Acta Polym.* 1986, **37**, 1
- 11 Kammer, H. W., Inoue, T. and Ougizawa, T. *Polymer* 1989, **30**, 888
- 12 Flory, P. J. *Disc. Faraday Soc.* 1970, **49**, 7
- 13 Manzini, G. and Crescenzi, V. *Macromolecules* 1975, **8**, 195
- 14 Kammer, H. W., Kressler, J., Kressler, B., Scheller, D., Kroschwitz, H. and Schmidt-Naake, G. *Acta Polym.* 1989, **40**, 75
- 15 Kressler, J., Kammer, H. W., Silvestre, C., DiPace, E., Cimmino, S. and Martuscelli, E. *Polym. Networks Blends* 1991, **1**, 225
- 16 Nojima, S., Watanabe, K., Zheng, Z. and Ashida, T. *Polym. J. (Tokyo)* 1988, **20**, 823
- 17 Li, W., Yan, R. and Jiang, B. *Polymer* 1992, **33**, 889
- 18 Defieuw, G., Groeninckx, G. and Reynaers, H. *Polym. Commun.* 1989, **30**, 267
- 19 Keith, H. D. and Padden, F. J. Jr *Polymer* 1984, **25**, 28